29th Congress of the International Council of the Aeronautical Sciences
St. Petersburg, Russia; September 7-12, 2014

DEVELOPMENT OF NEW PRELIMINARY DESIGN METHODOLOGIES FOR REGIONAL TURBOPROP AIRCRAFT BY CFD ANALYSES

Fabrizio Nicolosi*, Pierluigi Della Vecchia*, Danilo Ciliberti*, Vincenzo Cusati*
***Dept. of Industrial Engineering - University of Naples "Federico II"**
fabrizio.nicolosi@unina.it

Keywords: *Aircraft Design, Aerodynamics, CFD, Regional Turboprop*

Abstract

Since 2011 the aerodynamic research group of the Dept. of Industrial Engineering of the University of Naples "Federico II" makes use of the University's computing grid infrastructure SCoPE to perform parallel computing simulations with the commercial CAE package Star-CCM+. This infrastructure allows Navier-Stokes calculations on complete aircraft configurations in a relative short amount of time. Therefore, the software and the above mentioned infrastructure allow the parametric analysis of several configurations that are extremely useful to the correct estimation of aerodynamic interference among aircraft components and to highlight some useful trends that could indicate how a specific aerodynamic characteristic (i.e. the drag of a component, the wing downwash or the directional stability contribution of the vertical tail) is linked to aircraft geometrical parameters. Thus, with the choice of a specific set of test-cases it is possible to make a deep investigation on some aerodynamic features and, from the analyses of results, it is possible to extract and develop ad-hoc semi-empirical methodologies that could be used in preliminary design activities.

In this paper, two investigations are presented: the aerodynamic interference among aircraft components in sideslip and the aerodynamic characteristics of a fuselage, focusing on typical large turbopropeller aircraft category.

Nomenclature

A	aspect ratio
b	wing span
D	diameter
L	length
N	yawing moment
r	fuselage radius
S	planform area
Y	sideforce
z	vertical position of component
α	angle of attack
β	angle of sideslip
δ	angle of deflection of control surface
λ	taper ratio
Λ	sweep angle
ψ	windshield angle
θ	upsweep angle

Aerodynamic coefficients

C_D	drag coefficient
C_{M0}	pitching moment coefficient at $\alpha = 0$
$C_{M\alpha}$	pitch stability derivative
C_N	yawing moment coefficient

Capital letters

V	vertical tailplane
BV	vertical tail-fuselage combination
WBV	wing-fuselage-vertical tail comb.
WBVH	complete aircraft

Subscripts

f	fuselage
ftc or t	fuselage tailcone
h	horizontal tailplane
n	fuselage nose
r	rudder
v	vertical tailplane
w	wing

1 Introduction

Aircraft preliminary design often relies on statistics and semi-empirical methods. Most known references about the latter are the United States Air Force Data Compendium (USAF DATCOM) [1] and the Engineering Science Data Unit (ESDU) [2]. Both are based on the results of wind-tunnel tests performed by the National Advisory Committee for Aeronautics (NACA), which provided a huge amount of experimental data.

The geometries involved in those experimental investigations are quite different from nowadays airplane's geometry: elliptic-shaped fuselages, swept wing and tailplane planforms, not really similar to actual transport airplanes, see Figure 1 (ref. [3][4]). Also, different semi-empirical methods applied to the same aircraft configuration can lead to very different results, as highlighted in ref. [6], where the static stability derivatives provided by USAF DATCOM and ESDU about the vertical tail contribution to aircraft directional stability differ up to 25%, leading to a totally different tail design.

In recent works [5]-[8], a new approach to evaluate the static directional stability and control of a generic regional turboprop airplane has been developed by the authors, with the simulation of hundreds of different geometries and configurations in typical flight conditions with Reynolds-Averaged Navier-Stokes (RANS) equations. Results of the simulations have been collected in a "numerical database", with the aim to provide a simple and reliable procedure to follow both in aircraft preliminary design and analysis phases.

The idea of this approach is to highlight the aerodynamic interference among airplane components, changing fuselage shape, wing position and aspect ratio, vertical and horizontal tailplanes planforms and positions, as shown in Section 2.

This approach has been validated by other numerical simulations on several geometries, different from those used to develop the method, as shown in ref. [5].

Following the same approach, the authors have been recently focused on the estimation of fuselage drag and moment coefficients. Results of such investigations are published for the first time in this paper, as explained in Section 3.

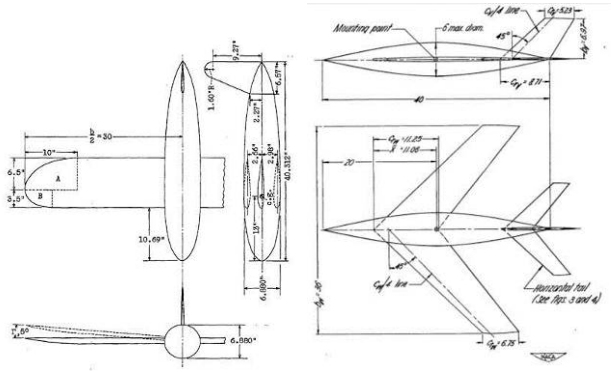

Figure 1 – NACA models (ref. [3][4]).

2 Evaluation of the aerodynamic interference effects in sideslip condition

2.1 Geometries investigated

The aircraft model has the typical characteristics (e.g. fuselage slenderness and lifting surfaces planform) of a regional turboprop airplane as highlighted in ref. [5]-[8]. Figure 2 shows a reference layout. Then, the aircraft components have been modified in size and position, which ranges are resumed in Table 1 and Table 2 to get more than a hundred of possible configurations. Also, Figure 3 shows the nomenclature for a generic planform (wing or tailplane).

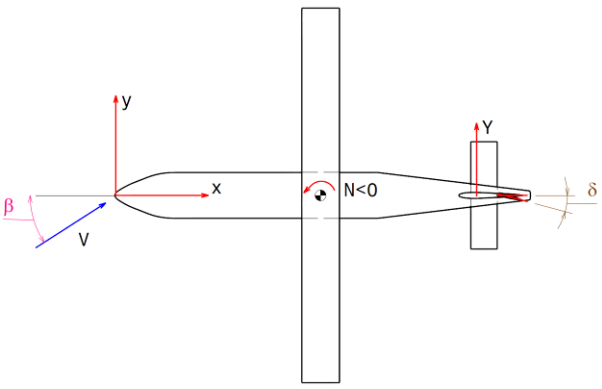

Figure 2 – Reference geometry.

Conf.	No. of sims	Changing parameters
V	~15	A_v, λ_v, Λ_v
BV	~30	A_v, λ_v, Λ_v, z_{ftc}/r
WBV	~50	A_v, A_w, z_w/r
WBVH	~65	A_v, z_h/b_{v1}, S_h/S_v

Table 1 – Possible aircraft components configurations.

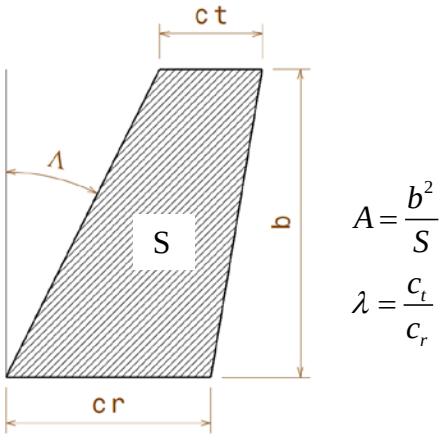

Figure 3 – Generic planform.

Parameter	Range
A_v	0.25 - 2.5
A_w	6 - 16
λ_v	0.3 - 1.0
Λ_v	0° - 60°
z_{ftc}/r	0 - 0.5
z_h/b_{v1}	0 - 1

Table 2 – Range of investigated parameters.

2.2 Numerical domain

The CAE package Star-CCM+ [9] has been used for the CFD simulations, most of which have been executed on the University's grid computing infrastructure (www.scope.unina.it) to perform parallel computations up to 128 CPUs for each run [10]. All simulations have been executed at 5° sideslip angle β and at 0° angle of attack α (with respect to the wing chord). The effect of the angle of attack on the yawing moment, at least in the linear range of the lift curve, is negligible [11]. The flow field is steady, subsonic, incompressible, and fully turbulent with Spalart-Allmaras model, demonstrated to be reliable at this flow condition [12][13].

2.3 The numerical approach

A detailed discussion of the numerical analyses set-up can be found in ref. [5] and [6], where meshes independence from number of cells, solution convergence and boundary layer phenomena (y+ ≈ 1) were well described.

The aerodynamic interference among airplane components is evaluated by the ratio of aerodynamic coefficients between two configurations, which differ for only one component. For instance, the effect of the fuselage on the vertical tail contribution to directional stability is given by the ratio C_{Nv} (BV) / C_{Nv} (V), where B stands for *body* (fuselage) and V stands for *vertical tailplane*. The effect of the *wing* (W) on the previous body-tail combination is given by the ratio C_{Nv} (WBV) / C_{Nv} (BV). Similarly, for the horizontal tailplane C_{Nv} (WBVH) / C_{Nv} (WBV). In this way, the global effect of the aerodynamic interference can be obtained by multiplying these factors

$$\frac{C_{N_v}(\mathrm{WBVH})}{C_{N_v}(\mathrm{WBV})} \cdot \frac{C_{N_v}(\mathrm{WBV})}{C_{N_v}(\mathrm{BV})} \cdot \frac{C_{N_v}(\mathrm{BV})}{C_{N_v}(\mathrm{V})} \quad (1)$$

2.4 Results and discussion

In this section, the interference effects among airplane components in sideslip are discussed. The most important contribution to aircraft directional stability and control is given by the vertical tailplane [14]-[17], but the response of the whole airplane to a directional gust (or a strong cross-wind force) also depends on the fuselage and (to a lesser extent) on the lifting surfaces.

2.4.1 Effect of the fuselage on the vertical tailplane in sideslip

This effect is measured by the ratio between the vertical tail yawing moment coefficient C_{Nv} (BV) of a body-tail configuration and that of the same vertical tailplane alone C_{Nv} (V).

The effect *of the fuselage on the vertical tail* in sideslip is to accelerate the flow in the region close to the tail-body junction. The aerodynamic interference depends on the ratio vertical tail span b_v to fuselage height $2r$ and on fuselage tailcone shape z_{ftc}/r see Figure 4. Tailplane planform has no effect, as shown in ref. [6] and [8]. The fuselage interference factor C_{Nv} (BV) / C_{Nv} (V) is shown in Figure 5. It is always greater than 1, so that the vertical tail yawing moment for a tail-body combination is always increased with respect to the isolated

vertical tailplane. This effect decreases with increasing $b_v/2r$ for a fuselage with a straight upper surface (red line in Figure 5), while it has a maximum for $b_v/2r = 3$ for the other fuselage geometries. Also, the interference effect decreases as the tailcone is lowered. It has to be noticed that typical fuselage – vertical tailplane geometries have a $b_v/2r$ ratio between 3.5 – 5.0 and a z_{ftc} / r ratio closer to 0.5 (see Figure 4).

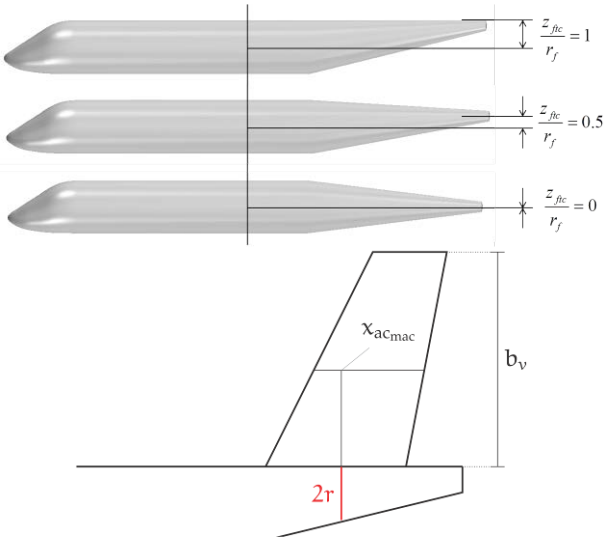

Figure 4 – Fuselage and vertical tail definitions.

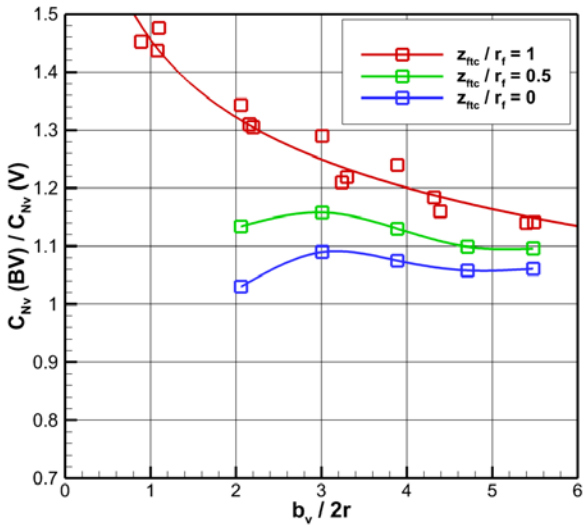

Figure 5 – Effect of the fuselage on the vertical tailplane

2.4.2 Effect of the vertical tail on the fuselage directional instability

The previous section has shown that the aerodynamic interference *of the fuselage on the vertical tail* is such that the vertical tail coupled with the fuselage *is more stable than the tail alone* (Figure 5), whereas the interference *of the vertical tail on the fuselage* is such that the fuselage coupled with the vertical tail *is less unstable than the fuselage alone*. In fact, as clearly shown in Figure 6, the ratio C_{Nf} (BV) / C_{Nf} (B) is less than 1 for all configurations. Also, it decreases with increasing $b_v/2r$ and by lowering the tailcone. According to the chart, a reduction of fuselage instability from 10% to 20% is expected for typical configurations ($b_v/2r \approx 3.5$).

By comparing both figures it is apparent that, for big tailplanes, it is not the fuselage that increases the stability contribution of the vertical tailplane, but it is the latter that reduces the instability of the former. Moreover both results shown in and Figure 6 and Figure 5 have inside the effect of the dynamic pressure usually takes into account with the term η_v.

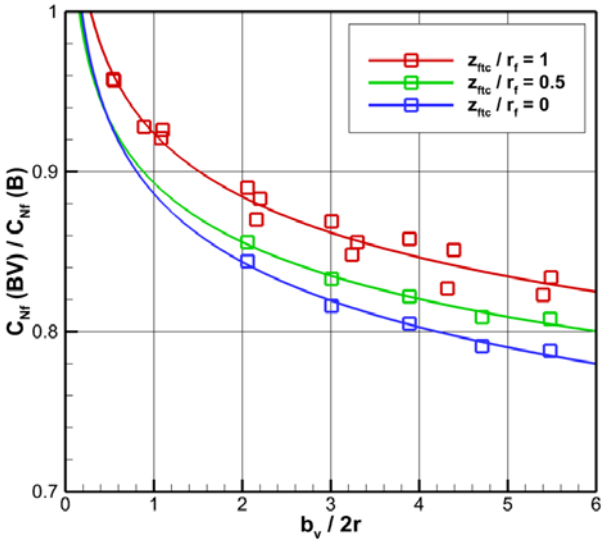

Figure 6 – Effect of the vertical tail on the fuselage.

2.4.3 Effect of the wing sidewash on the vertical tail in sideslip

In sideslip condition, the vertical position (high, mid, or low, see Figure 7) of the wing on the fuselage can increase or decrease the vertical tail contribution to yawing moment. It has been shown [6][8] that the effect of the wing aspect ratio is to decrease the interference factor up to 0.03 in the range 6-16, however an uncertainty of ±1% may be accounted for each wing position.

As shown in Figure 8, the low wing always increases the effectiveness of the vertical tail in sideslip, the mid wing is almost neutral, and the high wing decreases it. Also, lowering the fuselage tailcone (green line) increases the

interference effect between wing and vertical tailplane, but if it is too low (blue line) the dynamic pressure on the vertical tail drops, because of the adverse pressure gradients due to the fuselage shape, and the increase is less than expected. For typical turboprop configuration the sidewash effect is plus or minus 6-7% according to the wing position.

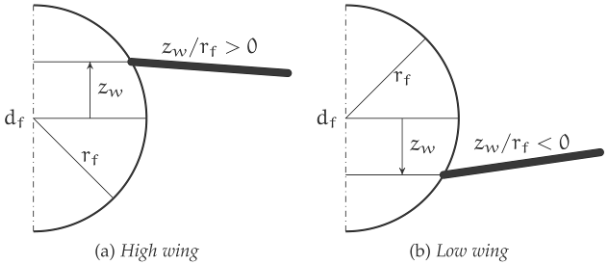

Figure 7 – Wing position definitions.

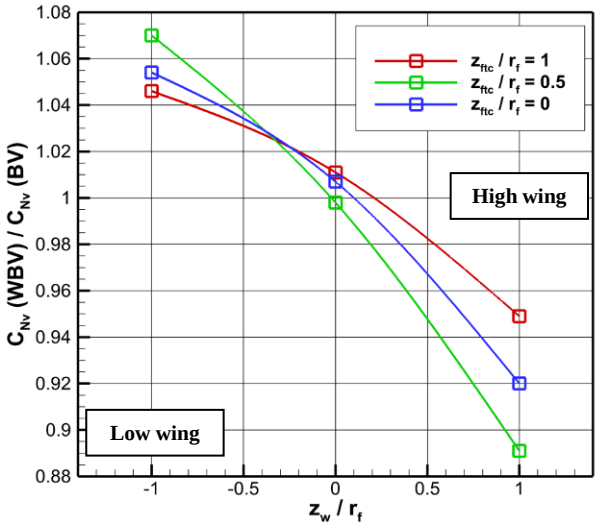

Figure 8 – Effect of the wing on the vertical tail.

2.4.4 Effect of the wing sidewash on the fuselage directional instability

The sidewash effect on the fuselage due to wing location is really strong (+15%) for high wing and high tailcones (Figure 9). In this case the wing wake affects the flow in the rear part of the fuselage, increasing its instability in sideslip. As in the case of longitudinal stability (see ref. [14]), the fuselage part behind the wing (and the center of gravity) has a stabilizing contribution that it is reduced if the airflow is disturbed (in this case aligned to the fuselage, reducing the sideslip angle of the rear fuselage zone).

A high wing with a low tailcone mitigates somewhat this effect, by taking the rear part of the fuselage off the wing wake. For the same reason, a low wing decreases the fuselage instability, but this effect is mostly 5% less than the tail-body combination without wing.

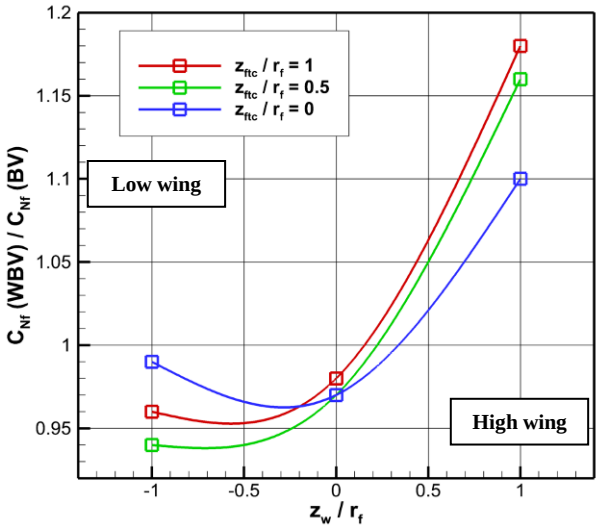

Figure 9 – Effect of the wing on the fuselage.

2.4.5 Effect of the horizontal tailplane on the vertical tailplane in sideslip

The sideforce developed in sideslip condition by the vertical tailplane increases if a horizontal tail is positioned on the vertical tail tip or it is mounted on the fuselage [6]-[8]. In both cases there is an *end-plate effect*. This is increased if the vertical tailplane aspect ratio is reduced and if the horizontal tail area is bigger than the vertical tail area (but in most cases this is negligible). The extreme low position (body-mounted horizontal tail) is favorable to structure and weight, whereas the extreme high position (T-tail) is favorable to aerodynamics. The choice of tail location depends on the wing position (to avoid the wing wake), engine location and on the class of airplane [16][17]. These effects are well depicted in Figure 10 and Figure 11, where it is evident that the extreme choices (body or T-tail) are favorable for directional stability. Cruciform vertical tail should be avoid if possible (especially in the z_h / b_{v1} range from 0.2 to 0.75).

2.4.6 Effect of the horizontal tailplane on the fuselage directional instability

For the configuration with z_{ftc} / r = 1 (straight upper surface) and A_v = 1.5, the effect of horizontal tail on the fuselage is shown in Figure 12. It can be seen that the horizontal

tailplane decreases the body directional instability if it is mounted on the fuselage. This can be considered as an end-plate effect, slightly intensifying as the horizontal tail is moved backward. The effect disappears as long as the horizontal tail is moved on the vertical tailplane

2.4.6 Effect of the directional control surface

On a conventional aircraft, the directional control is exerted by a rudder [1][16][17], that is a plain flap mounted on the vertical tailplane. The rudder has been realized by rotating the trailing edge of the vertical tail at 65% of the chord, obtaining a full span, no gap, directional control surface (Figure 13). Gap, overhang, and control surface effectiveness are not of interest in the analyses developed. In fact, their effects cancel each other in the interference factor derived to present results.

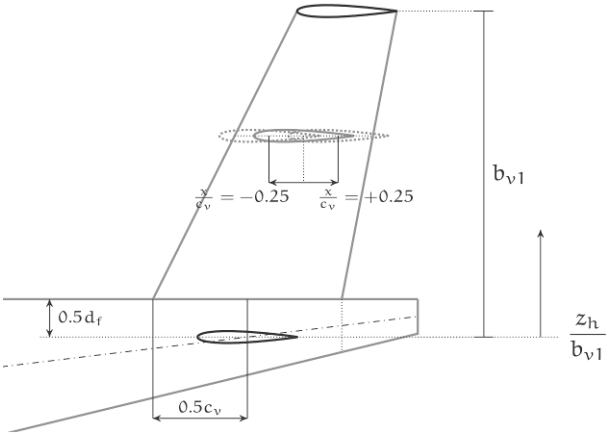

Figure 10 – Horizontal tailplane definitions.

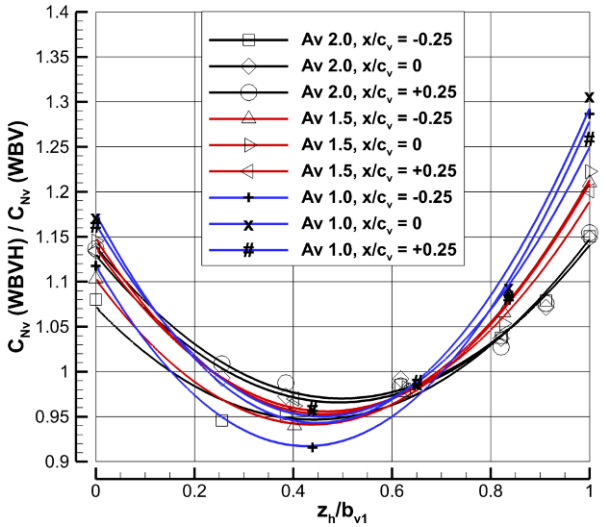

Figure 11 – Effect of the horizontal tail on the vertical tail.

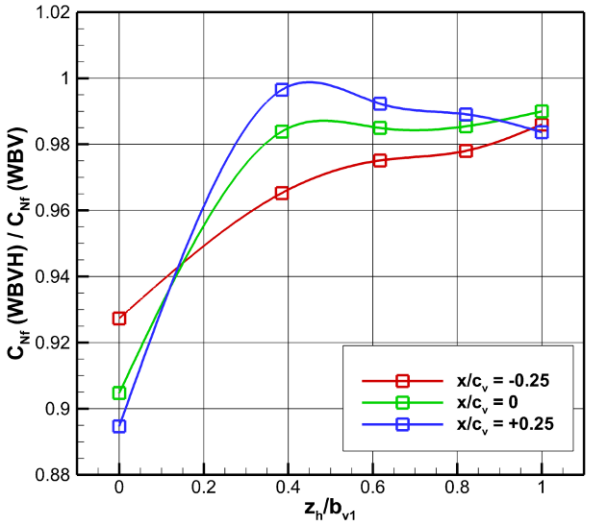

Figure 12 – Effect of the horizontal tail on the fuselage.

At zero sideslip, the deflection of the rudder creates a *local* sideslip angle due to the pressure changes on the surface of the vertical tailplane. Due to the induced circulation, the fuselage exerts an effect on the vertical tailplane, even if the airplane flight path is straight (for example at take-off). This interference is less than that predicted in sideslip. Wing has no effect, since it is located at distance from the tail-fuselage junction. The effect of the horizontal tailplane is similar, but less strong, to the one due to sideslip condition. Also, the authors have shown [7][8] that this interference effect is conserved at angles of sideslip, as shown in Figure 14, where the solid lines represent pure sideslip conditions, dashed lines represent sideslip angles combined with 10° of rudder deflection.

Figure 13 – Rudder deflection.

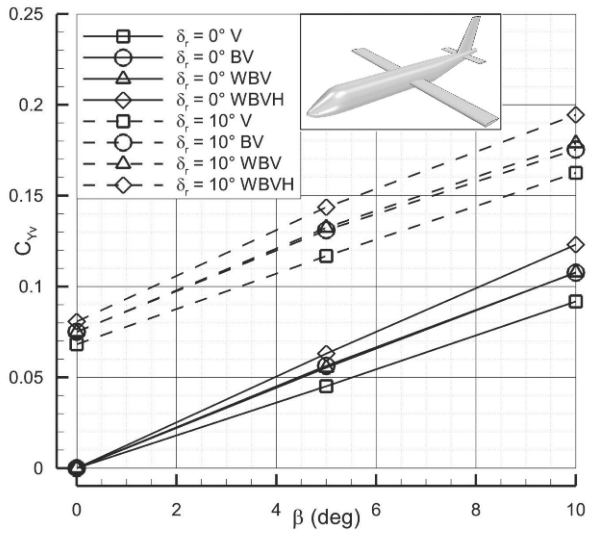

Figure 14 – Effect of the rudder deflection.

3 Evaluation of fuselage aerodynamic drag and pitching moment coefficients

Semi-empirical methods consider the drag coefficient as the sum of different contributions that can be evaluated by relations obtained from wind tunnel test which results are mainly collected in the USAF DATCOM database [1]. The total drag coefficient of an aircraft can be expressed as the sum of the zero lift drag coefficient and the drag-due-to-lift coefficient. This assumption is made when the approximation of a parabolic drag polar is assumed in order to estimate the drag coefficient for low incidence such as cruise and climb, that is until the lift coefficient becomes greater than 1. The zero lift drag coefficient is also known as parasite drag coefficient and it includes skin friction (function of wetted area), windshield ψ, upsweep θ, and base drag contributions, see Figure 15.

The semi-empirical methods are also used to predict the moment coefficient. One of the most used is the *strip-method*. It is so called because the fuselage is divided into strips each of which gives a contribution to pitching moment in a function of distance from the wing, see ref. [14].

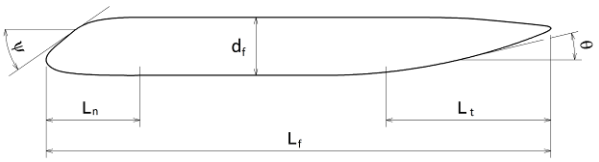

Figure 15 – Definitions for fuselage drag prediction.

3.1 The numerical approach

In this paper, a new approach is presented. From the reference layout shown in Figure 15, the nose, cabin (constant fuselage diameter), and tailcone geometry have been changed. Then, the aerodynamic drag, the pitching moment at zero incidence, and the longitudinal static stability derivative coefficients, C_D, C_{M0}, and $C_{M\alpha}$ respectively, have been evaluated. Fuselage lift coefficient is not presented due to the very low relevance in classical fuselage geometry design. Results are presented in terms of ratio of aerodynamic coefficients, which reference values are typical of a regional turboprop fuselage, as shown in Table 3.

$C_{D\,ref}$	$C_{M0\,ref}$	$C_{M\alpha\,ref}$ (deg^{-1})
0.0100	−0.050	0.030

Table 3 – Fuselage reference values.

3.1.1 Effect of nose slenderness ratio and windshield on drag and pitching moment coefficients

The nose of the reference layout has been changed in windshield angle ψ and slenderness L_n / D_f, see Figure 16. The windshield angle is related to pilot visibility and required by regulations (see for example CS 25.775 [18]). Cabin and tailcone have been held constant, thus the variation of the aerodynamic coefficient are due to the nose shape change. Results are shown from Figure 17 to Figure 19, where it can be seen that as the windshield angle increases, the drag coefficient C_D and the pitching moment coefficient C_{M0} increase too, because of adverse pressure gradients, whereas it has almost no effect on the longitudinal stability derivative $C_{M\alpha}$.

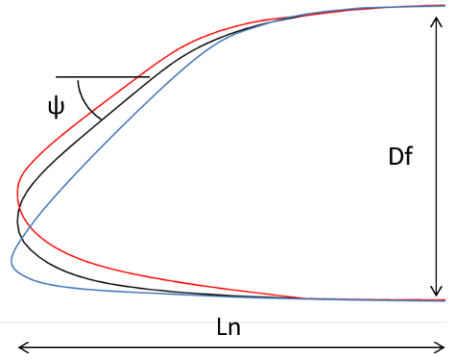

Figure 16 – Fuselage nose definitions.

For a given windshield angle, all the aerodynamic coefficients increases with increasing slenderness L_n / D_f, because of the bigger wetted area (noticed position of center of gravity in Figure 18). Moreover for a give fuselage nose slenderness the C_M at α=0 deg. can vary up to 40% in a feasible windshield angle range as shown in Figure 18.

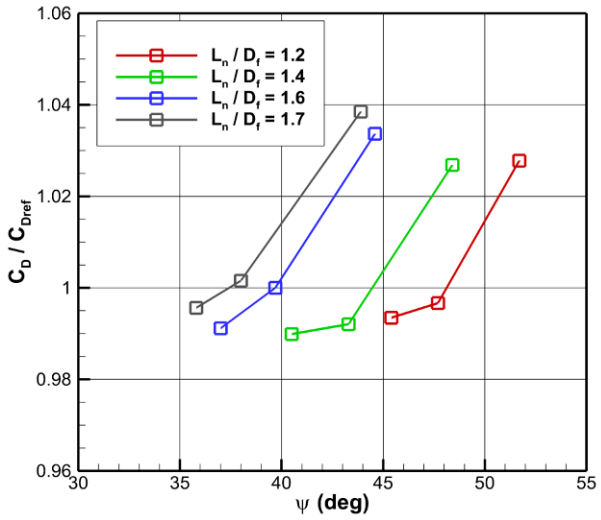

Figure 17 – Drag due to nose variation.

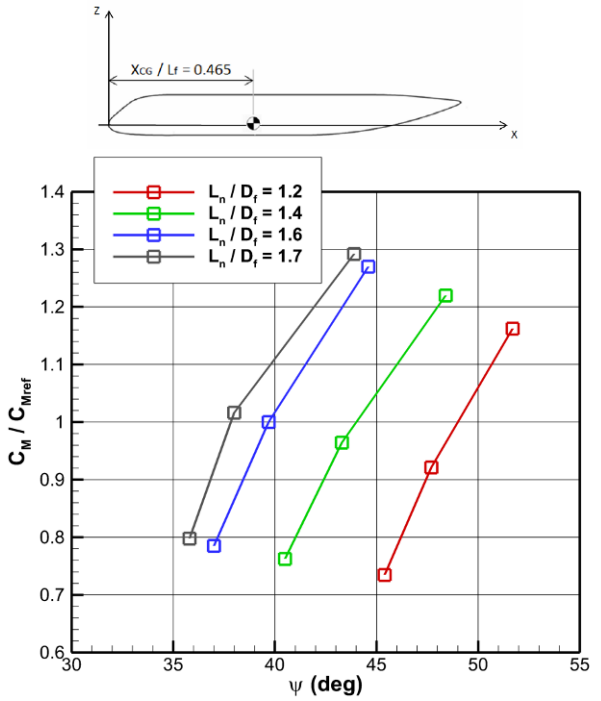

Figure 18 – Pitching moment at α = 0 due to nose variation.

3.1.2 Effect of cabin stretching

The cabin of the fuselage, which has a constant diameter, has been stretched, see Figure 20. As the slenderness ratio L_f / D_f increases so the wetted area does, thus the drag coefficient increases, see Figure 21. The pitching moment coefficient decreases, see Figure 22. The longitudinal instability increases too, see Figure 23.

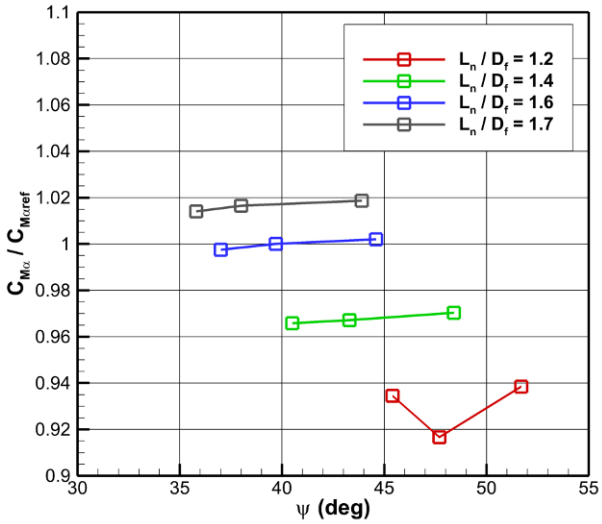

Figure 19 – Longitudinal instability due to nose variation.

3.1.3 Effect of tailcone slenderness ratio and upsweep on drag and pitching moment coefficients

The geometry of the tailcone has been changed in upsweep θ and slenderness L_t / D_f, see Figure 24. The upsweep angle is evaluated at the tail station which crosses the longitudinal nose axis at $x / L_f = 0.823$, as shown in Figure 25. It has been assumed this reference because the landing gear position and height may be unknown when evaluating fuselage aerodynamics in preliminary design and the tail lower surface may be curved.

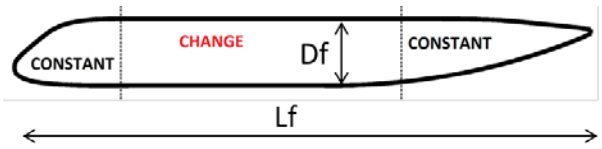

Figure 20 – Stretching of the fuselage cabin.

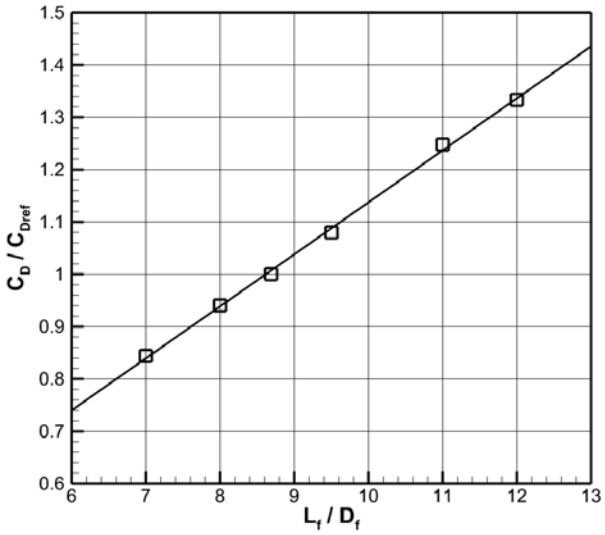

Figure 21 – Drag due to cabin stretching.

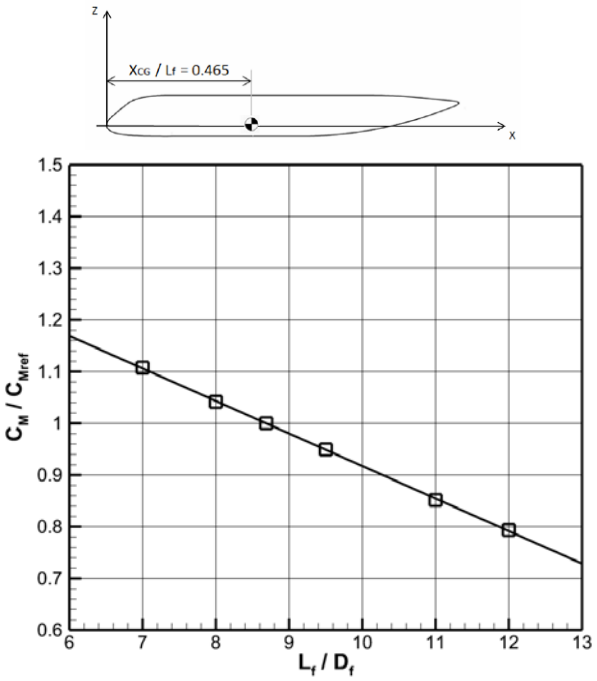

Figure 22 – Pitching moment due to cabin stretching.

As previously stated, the geometry of the other parts (nose and cabin) remains unchanged. For a given upsweep angle (Figure 26), the longer is the tail, the bigger is the drag coefficient. This is due to the increased wetted area. Conversely, for a given tailcone slenderness, the higher is the upsweep angle, the bigger is drag coefficient. In this last case, what is saved in skin friction (wetted area) is lost in pressure drag. The increase in upsweep angle leads to a slightly reduced longitudinal instability, see Figure 28. For a given upsweep angle, this instability increases with tail slenderness. However, the variation in $C_{M\alpha}$ are very small about 2-3%.

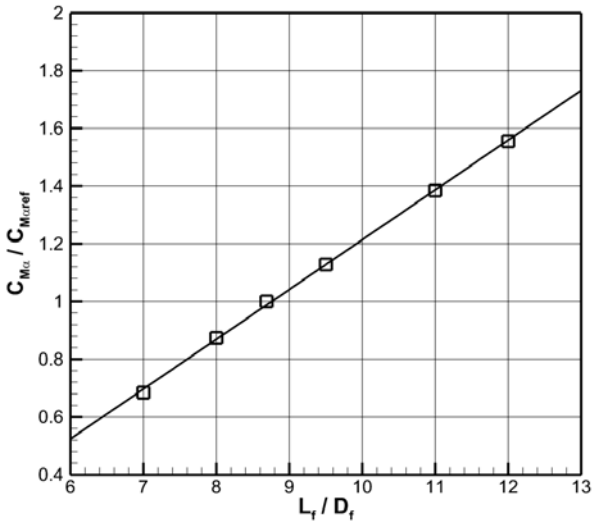

Figure 23 – Longitudinal instability due to cabin stretching.

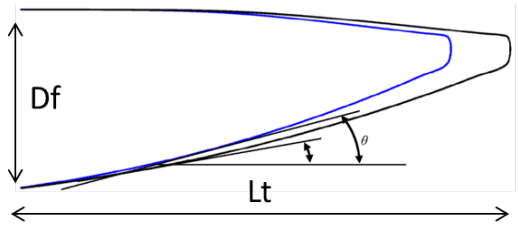

Figure 24 – Fuselage tailcone definitions.

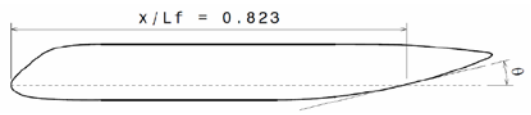

Figure 25 – Upsweep reference.

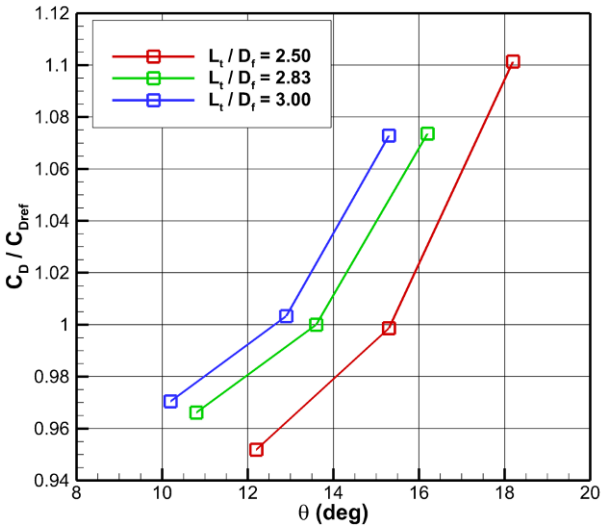

Figure 26 – Drag due to tail variation.

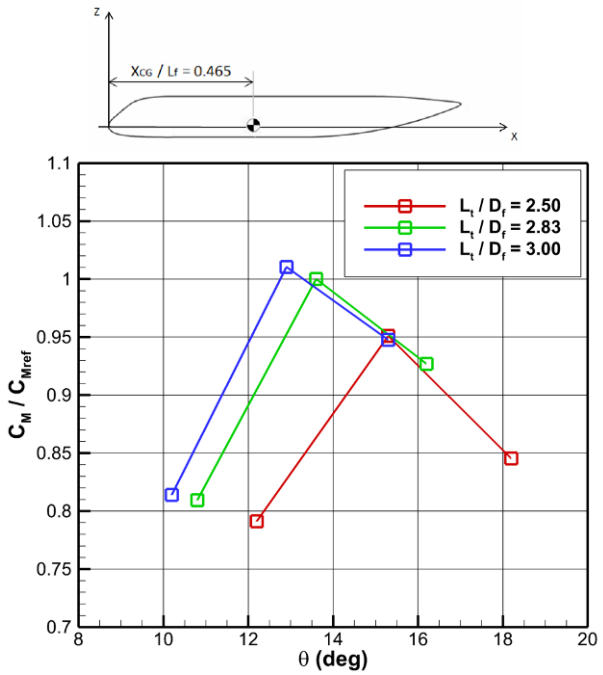

Figure 27 – Pitching moment due to tail variation.

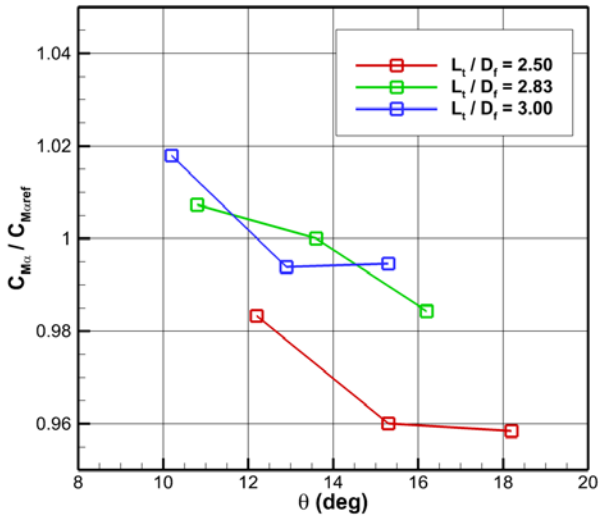

Figure 28 – Longitudinal instability due to tail variation.

4 Conclusion

This paper has shown the development of a numerical database about aerodynamic interference among aircraft components by deep investigations of numerous regional turboprop aircraft configurations. The massive use of a parallel computing on SCoPE [10] grid infrastructure made possible to get results of three-dimensional viscous simulations in a reasonable amount of time. The collected trends in aerodynamic coefficients against aircraft geometric parameters can be gathered to formulate new methodologies to estimate, in the presented cases, the contribution of the vertical tailplane and fuselage to aircraft directional stability and control, and the longitudinal aerodynamic characteristics (drag and pitching moments) of an isolated fuselage.

Some of these approaches (vertical tail stability and control) have already been validated and published [5]-[8].

It is the authors' opinion that these new methods can prove to be very accurate, since they are focused on a specific class of aircraft category (regional turboprop) and they have been developed and validated by CFD.

References

[1] Finck R D. *USAF stability and control DATCOM*. McDonnell Douglas Corporation, Wright-Patterson Air Force Base (Ohio, USA), 1978.

[2] Gilbey R W. *Contribution of fin to sideforce, yawing moment and rolling moment derivatives due to sideslip, (Yv)F, (Nv)F, (Lv)F, in the presence of body, wing and tailplane*. ESDU Item 82010, 1982.

[3] Bamber R J and House R O. *Wind-tunnel investigation of effect of yaw on lateral-stability characteristics. II–Rectangular NACA 23012 wing with a circular fuselage and a fin*. TN-730, National Advisory Committee for Aeronautics, 1939.

[4] Brewer J D and Lichtenstein J H. *Effect of horizontal tail on low-speed static lateral stability characteristics of a model having 45° sweptback wing and tail surfaces*. Technical Note 2010, National Advisory Committee for Aeronautics, 1950.

[5] Della Vecchia P, Development of Methodologies for the Aerodynamic Design and Optimization of New Regional Turboprop Aircraft, Doctoral Thesis in Aerospace, Naval and Quality Engineering, University of Naples, ISBN 978-88-98382-02-6.

[6] Nicolosi F, Della Vecchia P and Ciliberti D. An investigation on vertical tailplane contribution to aircraft sideforce. *Aerospace Science and Technology*, Vol. 28, pp. 401-416, 2013.

[7] Nicolosi F, Della Vecchia P and Ciliberti D. Aerodynamic interference issues in aircraft directional control. *Journal of Aerospace Engineering*, 2014.

[8] Ciliberti D, Nicolosi F and Della Vecchia P. A new approach in aircraft vertical tailplane design. *22th AIDAA Conference*, Napoli (Italy), Paper 034, 2013.

[9] Star-CCM+ Version 8.04.007-R8 User Guide, CD-adapco, 2013.

[10] SCoPE, Università degli studi di Napoli "Federico II", http://scope.unina.it/, 2012.

[11] Nicolosi F, Della Vecchia P and Corcione S. Aerodynamic analysis and design of a twin engine commuter aircraft. *28th ICAS Congress*, Brisbane (Australia), Paper ICAS 2012-1.6.2, 2012.

[12] Antunes A P, da Silva R G, Luiz J and Azevedo F. On the effects of turbulence modeling and grid refinement on high lift configuration aerodynamic simulations. in: *28th ICAS Congress*, Brisbane (Australia), 2012.
[13] Rumsey C L, Long M, Stuever R A and Wayman T R. *Summary of the First AIAA CFD High Lift Prediction Workshop*. AIAA-2011-839, American Institute of Aeronautics and Astronautics, 2011.
[14] Perkins C D and Hage R E. *Airplane Performance Stability and Control*. Wiley, New York, 1949.
[15] Obert E. *Aerodynamic design of transport aircraft*. Delft University Press, Delft, 2009.
[16] Torenbeek E. *Synthesis of subsonic airplane design*. Delft University Press, Delft, 1982.
[17] Raymer D P. *Aircraft design: a conceptual approach*. 3rd edition, AIAA, Washington, 1992.
[18] EASA. *Certification specifications and acceptable means of compliance for large aeroplanes CS-25*. European Aviation Safety Agency, Amendment 11, 4 July 2011.

Copyright Statement